COMPARATIVE ANALYSIS OF INFLUENZA MODEL SOLUTIONS USING EULER, HEUN, AND RK4 METHODS

Nabila Asyiqotur Rohmah[1)]
Mohamad Nur Fauzi[2)]
[1,2)]IAIN Ponorogo, Ponorogo, Indonesia
e-mail: annabila@iainponorogo.ac.id

ABSTRACT

This study explores the numerical solutions of an influenza epidemiological model, specifically the SEIR (Susceptible, Exposed, Infected, and Recovered) type, which is represented by a system of nonlinear differential equations. Three numerical methods were applied to solve this model: the Euler method, Heun's method, and the fourth-order Runge-Kutta (RK4) method. The solutions obtained from these numerical methods were compared to the reference solution from ODE45, as the exact solution of the SEIR model remains unknown. Numerical simulations revealed that using either a very large step size ($h = 0{,}5$) or a very small step size ($h = 0{,}001$) led to significant numerical errors. Among the five different step sizes tested, $h = 0{,}1$ provided the most accurate results. Based on the average computational time across different step sizes, the Euler method was the fastest, while RK4 was the slowest. However, the Euler method exhibited the largest error margin, whereas Heun's and RK4 methods produced comparable errors. Although Heun's method had the same error margin as RK4, it required less computational time, making it the most efficient choice for this case.

Keywords: Euler, Heun, influenza model, numerical method, Runge-Kutta.

INTRODUCTION

In the history of living creature, numerous diseases have emerged, some spreading widely and become epidemics affecting both human and animal population. Some of the most severe global outbreaks documented in history include: the polio epidemic in the United States in 1916 (Hv, 2014), the Ebola outbreak in West Africa from 2014 to 2016 (Kamorudeen et al., 2020), the COVID-19 pandemic beginning in 2020 (Wu et al., 2020), the HIV/AIDS pandemic worldwide (The Lancet, 2017), the Spanish influenza (Martini et al., 2019), the avian influenza (Charostad et al., 2023), the swine influenza (Mena et al., 2016), and the Hong Kong influenza (Jester et al., 2020). These diseases have spread on a large scale, with some still lacking a definitive cure.

Among the outbreaks, influenza is one the most frequently mentioned diseases. For human, influenza is highly contagious and potentially can lead to fatal outcomes in certain case. Its transmission is primarily caused by influenza viruses, which are RNA viruses belonging to the family *Orthomyxoviridae* (Liang, 2023). Influenza outbreaks typically occur during the winter season. The virus is spread through respiratory droplets expelled during when an infected person sneezes, coughs, or speaks (Richard & Fouchier, 2016). Symptoms of influenza include high fever, body aches, headaches, severe malaise, dry cough, sore throat, and runny nose (Moghadami, 2017). The virus can infect individuals across all age groups, from children to adults (Griggs et al., 2022).

To understand the dynamics of disease transmission, mathematical models can be employed, particularly for influenza. These models are referred to as mathematical epidemiological models. Numerous researchers have contributed to the development of epidemiological models for influenza. Notable studies include the SIRS-type influenza model incorporating vaccination strategies for susceptible individuals (Kharis & Cahyono, 2015), the mathematical analysis of an influenza A (H1N1) epidemic model with discrete delay (Krishnapriya et al., 2017), the modelling of the H5N1 influenza virus alongside optimal control strategies utilizing the Pontryagin maximum principle (Gourram et al., 2023), the modelling influenza A disease dynamics under Caputo-Fabizio fractional derivative with distinct contract rates (EVİRGEN et al., 2023), and an optimal control analysis for the H1N1 influenza model applying the Pontryagin minimum principle (Rahmadhania & Arif, 2020).

The epidemiological model can be characterized as a nonlinear system governed by first-order ordinary differential equations. Our focus is on solving the influenza model, which presents a nonlinear system coupled with an initial value problem. Obtaining exact solutions for nonlinear differential equations can be challenging; therefore, we employ numerical methods for this purpose. Three of famous numerical methods used are Euler, Heun, and fourth-order Runge-Kutta method. Some of notable work with these methods are: the test of stability and consistency of Heun method for SEIR type dengue fever (Novalia & Nasution, 2018); using Euler and Heun method to solve COVID-19 epidemiological model (Pratiwi & Mungkasi, 2021); using fourth-order Runge Kutta to solve monkeypox epidemiological model (Ludji & Buan, 2023), using fourth-order Runge-Kutta and Adam-Bashforth-Moulton to solve SIR epidemiological model (Setiawan & Mungkasi, 2021), using fourth-order Runge-Kutta to solve spreading of COVID-19 in Indonesia (Rahmadhani et al., 2023); using fourth-order and 45th order Runge-Kutta numerical method to solve influenza model (Mohammed & Mohammed, 2021) and using of Euler, Heun, and RK4 solutions to SEIR model for meningitis disease's spread (Hurit & Sudi Mungkasi, 2021).

In this study, we employ three well-established numerical methods: Euler, Heun, and the fourth-order Runge-Kutta method. Our objective is to compare these methods to determine which provides the fastest computation time and the lowest error margin, particularly in the case of the influenza model. To identify the method with the lowest error margin, we compare the numerical solutions with the reference solution obtained from the ODE45 algorithm in Python.

METHOD

Type of Research

This study applies two research approaches: numerical computation and simulation. In the numerical computation phase, three methods are applied: the Euler method, the Heun method, and the fourth-order Runge-Kutta method. Simulations are conducted to analyze the behavior of the influenza model. Additionally, we use the reference solution from the ODE45 algorithm in Python to compare it with the solutions obtained from these three numerical methods. The research process consists of the following steps:

1) Developing an SEIR-type influenza model;
2) Solving the model using the Euler, Heun, and fourth-order Runge-Kutta methods in Python;
3) Simulating the model with these numerical methods along with ODE45 in Python; and
4) Analyzing the results from the numerical solutions and simulations.

RESULTS AND DISCUSSION

SEIR Model for Influenza

In this study, we developed an epidemiological model for influenza using the assumptions outlined in Table 1. The model follows the SEIR type for influenza.

Table 1. Variables and Parameter Assumptions in SEIR Influenza model

Symbol	Description
$S(t)$	Susceptible population: Individuals who are healthy but at risk of being exposed to or infected by the influenza virus.
$E(t)$	Exposed population: Individuals who have been exposed to the influenza virus and are at risk of progressing to the infected state.
$I(t)$	Infected population: Individuals currently infected with influenza. Infected individuals may recover from the disease.
$R(t)$	Recovered population: Individuals who have recovered from influenza, transitioning from the exposed or infected state. Recovered individuals may return to the susceptible population over time.
β	Contact rate leading from the susceptible to the exposed population.
μ	Natural mortality rate
r	Birth rate
δ	Rate at which immunity is lost, leading recovered individuals to become susceptible again
σ	Average duration of the latent period before exposed individuals become infected.
κ	Recovery rate for the exposed population.
α	Influenza-induced mortality rate.
γ	Mean recovery time for infected population
N	Total population size.

Based on the information presented in Table 1, we can construct the compartment diagram shown in Figure 1 as follows:

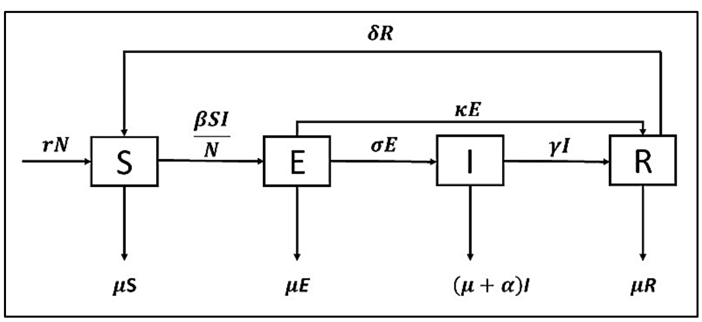

Figure 1. Compartment Diagram for SEIR Type Influenza Model

All parameters listed in Table 1 are assumed to be greater than zero. Based on these assumptions and the compartment diagram presented in Figure 1, we construct the mathematical model for the influenza disease as follows:

$$\frac{dS}{dt} = -\beta \frac{SI}{N} - \mu S + rN + \delta R \tag{1}$$

$$\frac{dE}{dt} = \beta\frac{SI}{N} - (\mu + \sigma + \kappa)E$$

$$\frac{dI}{dt} = \sigma E - (\mu + \alpha + \gamma)I$$

$$\frac{dR}{dt} = \kappa E + \gamma I - \mu R - \delta R$$

The total population *(N)* is defined as the sum of the susceptible, exposed, infected, and recovered populations. This relationship can be expressed mathematically using Equation (2).

$$N(t) = S(t) + E(t) + I(t) + R(t) \tag{2}$$

The total population derivative with respect to time can be determined from equation 2 as follow:

$$\frac{dN}{dt} = \frac{dS}{dt} + \frac{dE}{dt} + \frac{dI}{dt} + \frac{dR}{dt} = r - \mu N \qquad \text{or} \qquad \frac{dN}{dt} + \mu N = r \tag{3}$$

Equation (3) is a first-order linear equation. To solve it, we can multiply by an integrating factor and then integrate (Bronson & Costa, 2006). The form of Equation (3) with its integrating factor is shown in Equation (4).

$$e^{\mu t}\frac{dN(t)}{dt} + \mu e^{\mu t}N(t) = re^{\mu t} \quad \text{or} \quad \frac{d(e^{\mu t}N(t))}{dt} = re^{\mu t} \tag{4}$$

By applying integration to Equation (4), we arrive at the solution expressed in Equation (5):

$$N(t) = \frac{r}{\mu} + Ce^{-\mu t}\text{, with C is constant} \tag{5}$$

when $t = 0$, we can determine *C* as follows:

$$C = N(0) - \frac{r}{\mu}$$

This allows us to reformulate Equation (5) as

$$N(t) = \frac{r}{\mu} + \left(N(0) - \frac{r}{\mu}\right)e^{-\mu t}$$

This solution indicates that the total population is not constant but changes over time. In the limit as time approaches infinity $(t \to \infty)$, we find $\lim_{t\to\infty} N(t) = \frac{r}{\mu}$, This result implies that the total population converges to $\frac{r}{\mu}$.

Euler Method

The Euler method has a simple algorithm for computing numerical solutions. Euler method is first order method derived from linear term of Taylor series. The Euler method is also considered a first-order Runge-Kutta method.

Algorithm of Euler method (Munir, 2021):

$$k_1 = hf(x_n, y_n)$$

$$y_{n+1} = y_n + k_1$$

with h is interval length, $f(x_n, y_n)$ is differential value at (x_n, y_n), k_1 is predictor, y_n is value for n step, and y_{n+1} is prediction of next value.

With Euler method algorithm, the influenza model from equation (1) turn as follows:

$$S_{i+1} = S_i + ks_1 \tag{6}$$

$$E_{i+1} = E_i + ke_1 \tag{7}$$

$$I_{i+1} = I_i + ki_1 \tag{8}$$

$$R_{i+1} = R_i + kr_1 \tag{9}$$

with,

$$ks_1 = hf_1(t_i, S_i, I_i, R_i) = h\left(-\beta\frac{SI}{N} - \mu S + rN + \delta R\right)$$

$$ke_1 = hf_2(t_i, S_i, E_i, I_i) = h\left(\beta\frac{SI}{N} - (\mu + \sigma + \kappa)E\right)$$

$$ki_1 = hf_3(t_i, E_i, I_i) = h(\sigma E - (\mu + \alpha + \gamma)I)$$

$$kr_1 = hf_4(t_i, E_i, I_i, R_i) = h(\kappa E + \gamma I - \mu R - \delta R)$$

In this context S_{i+1}, E_{i+1}, I_{i+1}, R_{i+1} represent the equations used to calculate the number of individuals in the susceptible, exposed, infected, and recovered populations for the next iteration (or the following day). The term ks_1, ke_1, ki_1, kr_1 are derived from the Euler method and correspond to equations (6), (7), (8), and (9) in sequence.

Euler's method has local truncation error $O(h^2)$ and global truncation error $O(h)$. The truncation error derived from h interval length. The smaller value of h, the smaller error truncation in calculation.

Heun Method

The Heun method is a more complex algorithm than Euler's, as it is a modification of the Euler method. The heun's method used second order method to solve differential equation numerically. Heun's method can be derived from Taylor series with more term of Euler method. With the modification of Euler's, Heun's is more accurate algorithm. Heun's method can be described as a second-order Runge-Kutta method.

Algorithm of Heun method (Munir, 2021):

$$k_1 = hf(x_n, y_n)$$

$$k_2 = hf(x_n + h, y_n + k_1)$$

$$y_{n+1} = y_n + \frac{1}{2}(k_1 + k_2)$$

with h is interval length, $f(x_n, y_n)$ is differential value at (x_n, y_n), k_1 is predictor, k_2 is corrector for next value, y_n is value for n step, and y_{n+1} is prediction of next value.

With the Heun's method, Influenza model from equation (1) can be described as follow:

$$S_{i+1} = S_i + \frac{1}{2}(ks_1 + ks_2) \tag{10}$$

$$E_{i+1} = E_i + \frac{1}{2}(ke_1 + ke_2) \tag{11}$$

$$I_{i+1} = I_i + \frac{1}{2}(ki_1 + ki_2) \tag{12}$$

$$R_{i+1} = R_i + \frac{1}{2}(kr_1 + kr_2) \tag{13}$$

with,

$$ks_1 = hf_1(t_i, S_i, I_i, R_i) = h\left(-\beta\frac{SI}{N} - \mu S + rN + \delta R\right)$$

$$ke_1 = hf_2(t_i, S_i, E_i, I_i) = h\left(\beta\frac{SI}{N} - (\mu + \sigma + \kappa)E\right)$$

$$ki_1 = hf_3(t_i, E_i, I_i) = h(\sigma E - (\mu + \alpha + \gamma)I)$$

$$kr_1 = hf_4(t_i, E_i, I_i, R_i) = h(\kappa E + \gamma I - \mu R - \delta R)$$

$$ks_2 = h\left(-\frac{\beta}{N}(S_i + hks_1)(I_i + hki_1) - \mu(S_i + hks_1) + rN + \delta(R_i + hkr_1)\right)$$

$$ke_2 = h\left(-\frac{\beta}{N}(S_i + hks_1)(I_i + hki_1) - (\mu + \sigma + \kappa)(E_i + hke_1)\right)$$

$ki_2 = h\big(\sigma(E_i + hke_1) - (\mu + \alpha + \gamma)(I_i + hki_1)\big)$

$ks_2 = h\big(\kappa(E_i + hke_1) + \gamma(I_i + hki_1) - \mu(R_i + hkr_1) - \delta(R_i + hkr_1)\big)$

Similar to Euler method, in this context S_{i+1}, E_{i+1}, I_{i+1}, R_{i+1} represent the equations used to calculate the number of individuals in the susceptible, exposed, infected, and recovered populations for the next iteration (or the following day). The term $ks_1, ke_1, ki_1, kr_1, ks_2, ke_2, ki_2, kr_2$are derived from the Heun method and correspond to equations (10), (11), (12), and (13) in sequence.

Heun's method has a local truncation error $O(h^3)$ and global truncation error $O(h^2)$. Theoretically, Heun has less error than Euler method.

Fourth-order Runge-Kutta Method

The Runge-Kutta method is widely used to solve both linear and nonlinear differential equations. In this study, we applied the fourth-order Runge-Kutta (RK4) method to compare with the Euler and Heun methods.

Algorithm of RK4 method (Munir, 2021):

$k_1 = hf(x_n, y_n)$

$k_2 = hf(x_n + \frac{1}{2}h, y_n + \frac{1}{2}k_1)$

$k_3 = hf(x_n + \frac{1}{2}h, y_n + \frac{1}{2}k_2)$

$k_4 = hf(x_n + h, y_n + k_3)$

$y_{n+1} = y_n + \frac{1}{6}(k_1 + 2k_2 + 2k_3 + k_4)$

with the RK4 method, influenza model from equation (1) can be described as follow:

$$S_{i+1} = S_i + \frac{1}{6}(ks_1 + 2ks_2 + 2ks_3 + ks_4) \quad (14)$$

$$E_{i+1} = E_i + \frac{1}{6}(ke_1 + 2ke_2 + 2ke_3 + ke_4) \quad (15)$$

$$I_{i+1} = I_i + \frac{1}{6}(ki_1 + 2ki_2 + 2ki_3 + ki_4) \quad (16)$$

$$R_{i+1} = R_i + \frac{1}{6}(kr_1 + 2kr_2 + 2kr_3 + kr_4) \quad (17)$$

With,

$ks_1 = hf_1(t_i, S_i, I_i, R_i) = h\left(-\beta\frac{SI}{N} - \mu S + rN + \delta R\right)$

$ke_1 = hf_2(t_i, S_i, E_i, I_i) = h\left(\beta\frac{SI}{N} - (\mu + \sigma + \kappa)E\right)$

$$ki_1 = hf_3(t_i, E_i, I_i) = h(\sigma E - (\mu + \alpha + \gamma)I)$$

$$kr_1 = hf_4(t_i, E_i, I_i, R_i) = h(\kappa E + \gamma I - \mu R - \delta R)$$

$$ks_2 = hf\left(t_i + \frac{h}{2}, S_i + \frac{h}{2}ks_1, I_i + \frac{h}{2}ki_1, R_i + \frac{h}{2}kr_1\right)$$
$$= h\left(-\frac{\beta}{N}\left(S_i + \frac{h}{2}ks_1\right)\left(I_i + \frac{h}{2}ki_1\right) - \mu\left(S_i + \frac{h}{2}ks_1\right) + rN + \delta\left(R_i + \frac{h}{2}kr_1\right)\right)$$

$$ke_2 = hf\left(t_i + \frac{h}{2}, S_i + \frac{h}{2}ks_1, E_i + \frac{h}{2}ke_1, I_i + \frac{h}{2}ki_1\right)$$
$$= h\left(-\frac{\beta}{N}\left(S_i + \frac{h}{2}ks_1\right)\left(I_i + \frac{h}{2}ki_1\right) - (\mu + \sigma + \kappa)\left(E_i + \frac{h}{2}ke_1\right)\right)$$

$$ki_2 = hf(t_i + \frac{h}{2}, E_i + \frac{h}{2}ke_1, I_i + \frac{h}{2}ki_1) = h\left(\sigma\left(E_i + \frac{h}{2}ke_1\right) - (\mu + \alpha + \gamma)\left(I_i + \frac{h}{2}ki_1\right)\right)$$

$$ks_2 = hf\left(t_i + \frac{h}{2}, E_i + \frac{h}{2}ke_1, I_i + \frac{h}{2}ki_1, R_i + \frac{h}{2}kr_1\right)$$
$$= h\left(\kappa\left(E_i + \frac{h}{2}ke_1\right) + \gamma\left(I_i + \frac{h}{2}ki_1\right) - \mu\left(R_i + \frac{h}{2}kr_1\right) - \delta\left(R_i + \frac{h}{2}kr_1\right)\right)$$

$$ks_3 = hf\left(t_i + \frac{h}{2}, S_i + \frac{h}{2}ks_2, I_i + \frac{h}{2}ki_2, R_i + \frac{h}{2}kr_2\right)$$
$$= h\left(-\frac{\beta}{N}\left(S_i + \frac{h}{2}ks_2\right)\left(I_i + \frac{h}{2}ki_2\right) - \mu\left(S_i + \frac{h}{2}ks_2\right) + rN + \delta\left(R_i + \frac{h}{2}kr_2\right)\right)$$

$$ke_3 = hf\left(t_i + \frac{h}{2}, S_i + \frac{h}{2}ks_2, E_i + \frac{h}{2}ke_2, I_i + \frac{h}{2}ki_2\right)$$
$$= h\left(-\frac{\beta}{N}\left(S_i + \frac{h}{2}ks_2\right)\left(I_i + \frac{h}{2}ki_2\right) - (\mu + \sigma + \kappa)\left(E_i + \frac{h}{2}ke_2\right)\right)$$

$$ki_3 = hf(t_i + \frac{h}{2}, E_i + \frac{h}{2}ke_2, I_i + \frac{h}{2}ki_2) = h\left(\sigma\left(E_i + \frac{h}{2}ke_2\right) - (\mu + \alpha + \gamma)\left(I_i + \frac{h}{2}ki_2\right)\right)$$

$$ks_3 = hf\left(t_i + \frac{h}{2}, E_i + \frac{h}{2}ke_2, I_i + \frac{h}{2}ki_2, R_i + \frac{h}{2}kr_2\right)$$
$$= h\left(\kappa\left(E_i + \frac{h}{2}ke_2\right) + \gamma\left(I_i + \frac{h}{2}ki_2\right) - \mu\left(R_i + \frac{h}{2}kr_2\right) - \delta\left(R_i + \frac{h}{2}kr_2\right)\right)$$

$$ks_4 = hf(t_i + h, S_i + hks_3, I_i + hki_3, R_i + hkr_3)$$

$$= h\left(-\frac{\beta}{N}(S_i + hks_3)(I_i + hki_3) - \mu(S_i + hks_3) + rN + \delta(R_i + hkr_3)\right)$$

$$ke_4 = hf(t_i + h, S_i + hks_3, E_i + hke_3, I_i + hki_3)$$
$$= h\left(-\frac{\beta}{N}(S_i + hks_3)(I_i + hki_3) - (\mu + \sigma + \kappa)(E_i + hke_3)\right)$$

$$ki_4 = hf(t_i + h, E_i + hke_3, I_i + hki_3) = h\big(\sigma(E_i + hke_3) - (\mu + \alpha + \gamma)(I_i + hki_3)\big)$$

$$kr_4 = hf(t_i + h, E_i + hke_3, I_i + hki_3, R_i + hkr_3)$$
$$= h\big(\kappa(E_i + hke_3) + \gamma(I_i + hki_3) - \mu(R_i + hkr_3) - \delta(R_i + hkr_3)\big)$$

Like Euler and Heun method, in this context S_{i+1}, E_{i+1}, I_{i+1}, R_{i+1} represent the equations used to calculate the number of individuals in the susceptible, exposed, infected, and recovered populations for the next iteration (or the following day). The term ks_1, ke_1, ki_1, kr_1, ks_2, ke_2, ki_2, kr_2, ks_3, ke_3, ki_3, kr_3, ks_4, ke_4, ki_4, kr_4 are derived from the RK4 method. The term ks_1, ks_2, ks_3, ks_4 are derived to correspond to equations (14), the term ke_1, ke_2, ke_3, ke_4 are derived to correspond to equations (15), the term ki_1, ki_2, ki_3, ki_4 are derived to correspond to equations (16), and the term kr_1, kr_2, kr_3, kr_4 are derived to correspond to equations (17) in sequence.

Numerical Computation and Simulation

In this section, we present the results of the computations and simulations using Python. The initial values and parameter settings for the simulation are provided in Table 2. The initial values S_0, E_0, I_0, R_0 were assumed, and the parameter values were taken from (Mohammed & Mohammed, 2021). The simulation was run for 200 days with three interval time steps of h (0,1; 0,01; and 0,2).

Table 2. Variables and Parameters Value

Parameters	Value of parameters	Unit	Source
β	0.5020000	/day	Mohammed & Mohammed, 2021
μ	0.0003671	/day	Mohammed & Mohammed, 2021
r	0.0006762	/day	(Mohammed & Mohammed, 2021)
δ	0.0027400	/day	(Mohammed & Mohammed, 2021)
σ	0.6990000	/day	Mohammed & Mohammed, 2021
κ	0.0001500	/day	Mohammed & Mohammed, 2021
α	0.0300000	/day	Mohammed & Mohammed, 2021
γ	0.3600000	/day	Mohammed & Mohammed, 2021
S_0	40	individu	Assumption
E_0	15	individu	Assumption
I_0	25	individu	Assumption
R_0	20	individu	Assumption

This section presents three figures from the simulation. Figure 2 through 4 compare of the solutions obtained from the ODE45, Euler, Heun, and RK4 numerical methods, with each compartment displayed in separate subplots for clearer analysis. Each figure uses a different time step: Figure 2 uses $h = 0{,}2$; Figure 3 uses $h = 0{,}1$; and Figure 4 uses $h = 0{,}01$. The ODE45 algorithm is used as a reference since the exact analytical solution for the SEIR model remains unknown. We set the relative tolerance and absolute tolerance $2{,}3 \times 10^{-14}$ for ODE45, as the value is close enough to minimum allowable value for ODE45 algorithm in Python, which is $2.220446049250313 \times 10^{-14}$. These tolerance values were chosen to ensure that the reference solution from ODE45 is accurate and reliable.

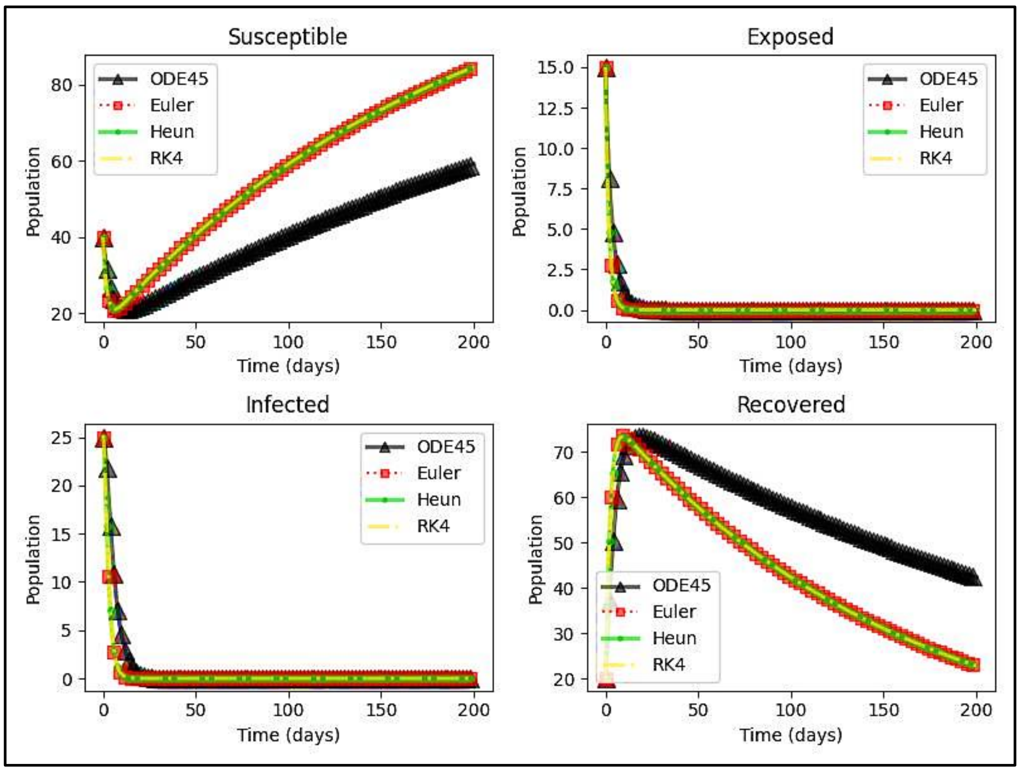

Figure 2. Simulation of SEIR Type Influenza Model with ODE45, Euler, Heun, and RK4 Method with $\boldsymbol{h = 0,2}$

Figure 2 separates the graphs for each compartment (Susceptible, Exposed, Infected, Recovered) to illustrate the solutions obtained from ODE45, Euler, Heun, and RK4. Here the analysis of simulation:

1. Susceptible graph: All numerical methods (Euler, Heun, and RK4) produce similar results, showing an initial decrease in the susceptible population during the first few days, followed by a consistent increase over time. This trend is primarily due to recovery processes and population growth from the birth rate (r). Over time, all numerical methods gradually diverge from the ODE45 solution.
2. Exposed graph: All methods consistently predict a sharp decline in the exposed population early in the simulation, reaching very low values around day 20 and eventually stabilizing near zero. The ODE45 solution and numerical methods overlap after reaching these low values.

3. Infected graph: All methods show a decreasing trend in the infected population, eventually approaching zero. The numerical solutions closely follow the ODE45 solution.
4. Recovered graph: The recovered population follows a similar trend across all methods, initially increasing and then gradually decreasing after reaching its peak. This decline occurs as the number of infected individuals decreases. Over time, all numerical methods diverge from the ODE45 solution.

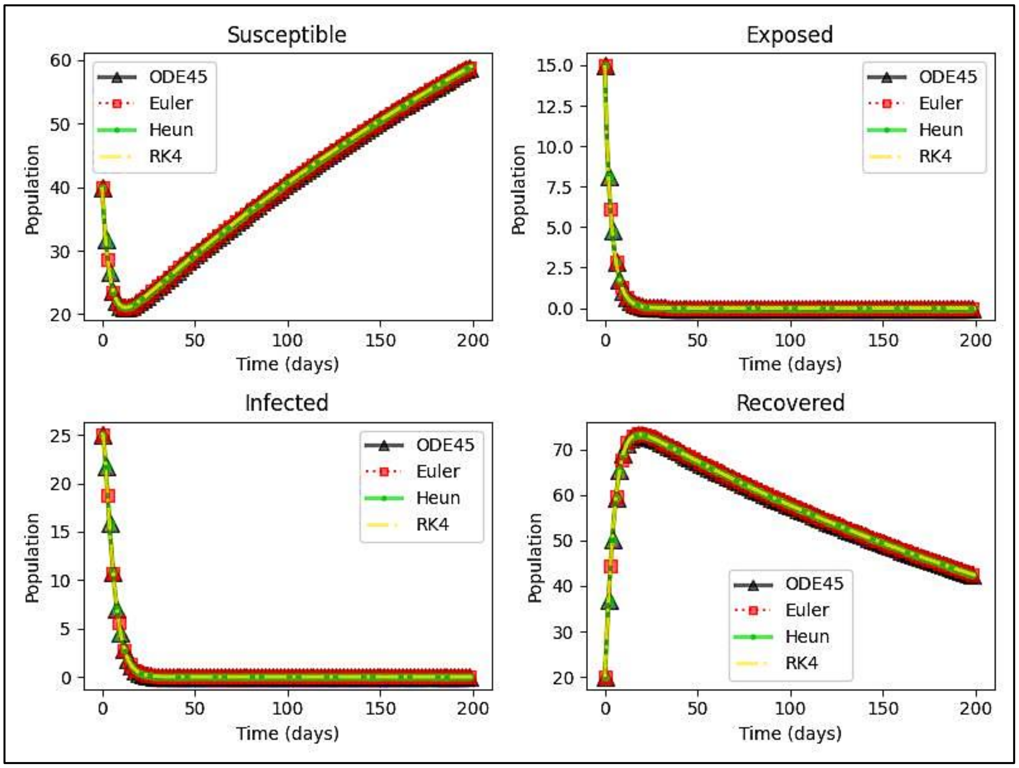

Figure 3. Simulation of SEIR Type Influenza Model with ODE45, Euler, Heun, and RK4 Method with $h = 0,1$

Figure 3 presents separate graphs for each compartment (Susceptible, Exposed, Infected, Recovered) and compares the results of different methods: ODE45, Euler, Heun, and RK4. Below is the analysis of the simulation:

1. Susceptible graph: All methods produce highly similar results, showing a consistent trend of an increasing susceptible population over time after an initial decline in the first few days. After days 12–13, the susceptible population increases rapidly.
2. Exposed graph: All methods consistently predict a sharp decline in the exposed population early in the simulation, reaching very low values after 20 days.
3. Infected graph: All methods demonstrate that the infected population decrease from day 1 to nearly zero.
4. Recovered graph: the trend of the recovered population shows comparable increases across all methods, followed by a gradual decrease after reaching its peak at day 18-19. The number of

recovered individuals declines because there are no longer infected individuals available to recover.

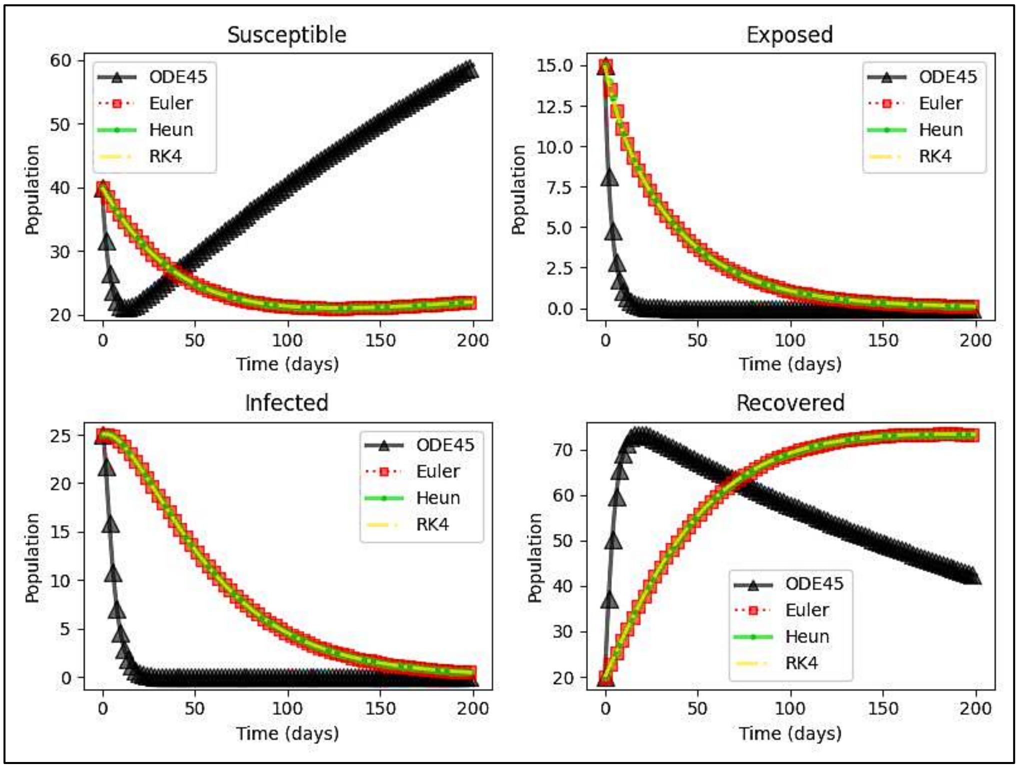

Figure 4. Simulation of SEIR Type Influenza Model with ODE45, Euler, Heun, and RK4 Method with $h = 0,01$

Figure 4 illustrates separate plots for each compartment (Susceptible, Exposed, Infected, Recovered) to present the simulation results from different methods: ODE45, Euler, Heun, and RK4. The following is an analysis of the simulation results:

1. Susceptible graph: All numerical methods (Euler, Heun, and RK4) produce similar results, showing a consistent trend of a slow increase in the susceptible population over time after an initial decline in the first 100 days. Over time, all numerical methods diverge significantly from the ODE45 solution, where the numerical methods predict populations near zero, whereas ODE45 projects a continuous increase.
2. Exposed graph: All methods consistently predict a sharp decline in the exposed population early in the simulation, reaching very low values around day 10 and eventually stabilizing near zero. The graphs of the ODE45 solution and numerical methods overlap after reaching these low values.
3. Infected graph: All methods show a rapid decline in the infected population, approaching nearly zero by day 20. The numerical solutions closely follow the ODE45 solution.
4. Recovered graph: The trend of the recovered population shows comparable increases across all numerical methods, followed by a gradual decrease after reaching its peak. Over time, all numerical method graphs diverge from the ODE45 solution, where the numerical methods predict a slow

decrease after day 180, whereas ODE45 predicts a sharp drop in the recovered population after day 20.

From simulations in Figure 2-4, all methods (ODE45, Euler, Heun, and RK4) show similar behaviour in modelling influenza dynamics. However, the accuracy of numerical methods depends on the time step size. With time step $h = 0{,}1$, Figure 3 shows that the ODE45 solution graph slightly close to all numerical method graph. On the contrary, for larger ($h = 0{,}2$ in Figure 2) and smaller ($h = 0{,}01$ in Figure 4) time steps, the ODE45 solutions for the susceptible and recovered compartments deviate significantly from the numerical solutions, indicating higher numerical errors. This suggests that selecting an appropriate time step is crucial for achieving accurate numerical approximations.

Table 3 presents the mean error tabulation for the solutions obtained from the Euler, Heun, and RK4 methods compared to ODE45 solution over the first 200 days of simulation. We use five different time step sizes ($h = 0{,}5;\ 0{,}2;\ 0{,}1;\ 0{,}01; 0{,}001$) to assess consistency of numerical method based on various time step sizes.

Table 3. Mean Error of Euler, Heun, and RK4 compared to ODE45 Solution

h **step size**	**Method**	**Variable**			
		Susceptible	**Exposed**	**Infected**	**Recovered**
0,5	Euler	12,73233	10,77759	23,13808	28,47393
	Heun	12,73201	10,77819	23,13748	28,47434
	RK4	12,73201	10,77818	23,13748	28,47434
0,2	Euler	16,58304	0,138288	0,407288	13,91492
	Heun	16,63231	0,134803	0,401667	13,94410
	RK4	16,63184	0,134902	0,401643	13,94380
0,1	Euler	0,055785	0,003236	0,006700	0,057456
	Heun	0,009625	0,000182	0,000415	0,008492
	RK4	0,009775	0,000135	0,000402	0,008587
0,01	Euler	19,33680	2,403618	7,130431	19,72220
	Heun	19,32983	2,406811	7,135293	19,71715
	RK4	19,32983	2,406807	7,135294	19,71715
0,001	Euler	38,15406	0,317895	0,825156	30,56113
	Heun	37,38100	0,311924	0,815500	29,52708
	RK4	37,39202	0,312250	0,815429	29,54330

Table 3 also compares the mean error for all numerical methods for five different time step sizes. When $h = 0{,}1$, the errors from Heun and RK4 are nearly identical, meanwhile Euler's method exhibits the highest error. Simulations with $h = 0{,}5; 0{,}2; 0{,}01;$ and $0{,}001$ indicate that the errors from all three numerical method are not significantly different. Although $h = 0{,}001$ is smallest time step, it does not present the most accurate results; instead, it leads to increased numerical errors compared to $h = 0{,}1$, suggesting that $h = 0{,}1$ provides the best accuracy.

The results of mean error for numerical method from Table 3 indicates that $h = 0{,}1$ provides the most accurate solution compared to smaller and larger time steps. This observation can be explained by several numerical factors, including rounding error, truncation error, and numerical stability, as discussed below (Chapra & Canale, 2015):

1. Accumulation of rounding error: Smaller h values require significantly more iterations. Each iteration produces minor rounding error from computation, especially with floating-point number type. When h is very small, the accumulation of these rounding error from significant iterations potentially reduces the computational accuracy.
2. Optimal h value for balancing accuracy and efficiency: All three numerical methods produces both truncation error and rounding error. When h is too small, rounding errors increased, meanwhile h is too large results in higher truncation errors. In this case, $h = 0{,}1$ likely the optimal interval that balances both truncation and rounding errors.
3. Numerical stability issues: The Euler, Heun, and RK4 methods are explicit numerical schemes, which may exhibit numerical instability under certain conditions. Since Euler and Heun are first order and second order of Runge-Kutta, they share similar error characteristics.

Table 4 summarizes the execution times for each method across three interval settings. The algorithms run in Python using Visual Studio Code, with four repeated trials for each method.

Table 4. Execution Times of Euler, Heun, and RK4 (in second)

h step sizes	Method	Trial Number				Mean
		1	2	3	4	
0,5	Euler	0,024176121	0,015631199	0,015628815	0,015630007	0,017766536
	Heun	0,025823116	0,026811123	0,038139343	0,033630371	0,031100988
	RK4	0,068858385	0,055656672	0,051197529	0,056714058	0,058106661
0,2	Euler	0,045193434	0,013328075	0,012529850	0,016000509	0,021762967
	Heun	0,047188759	0,045158625	0,050793648	0,040214300	0,045838833
	RK4	0,086301804	0,089160681	0,128798962	0,083012819	0,096818567
0,1	Euler	0,011697054	0,009056330	0,012862921	0,014721870	0,012084544
	Heun	0,052272797	0,047997236	0,036287785	0,035549164	0,043026746
	RK4	0,079683781	0,085564852	0,066128492	0,091261864	0,080659747
0,01	Euler	0,011799574	0,015130520	0,012326479	0,018214226	0,014367700
	Heun	0,042677879	0,047042847	0,068734646	0,051344633	0,052450001
	RK4	0,077005148	0,113099337	0,126967192	0,117500067	0,108642936
0,001	Euler	0,033812046	0,021074772	0,006532907	0,027625561	0,022261322
	Heun	0,063572645	0,035370588	0,056935549	0,052709818	0,052147150
	RK4	0,140364885	0,105368614	0,115224838	0,109085560	0,117510974

Across all running tests (1-4) in Table 4, the Euler method consistently proves to be the fastest algorithm, while RK4 requires more time to execute compared to the other methods. For each method, an interval of $h = 0{,}1$ results in the shortest execution time.

According to the simulations, using an interval of h=0,1 provides the most accurate calculation. The error margins for Heun and RK4 are comparable. Across all test, $h = 0{,}1$ also minimizes computation time. Euler is fastest method meanwhile RK4 is slowest. Considering both execution time and mean error, Heun proves to be the most efficient algorithm for this case, as its effectiveness computation time and accurateness compared to RK4.

CONCLUSION

Based on the result and discussion, the conclusions of this study are:

1. Among the tested time steps, $h = 0{,}1$ offers the most accurate result for Euler, Heun, and RK4, reducing numerical errors compare to other time step sizes. Very large ($h = 0{,}5$) or very small ($h = 0{,}001$) time steps result in numerical inconsistencies because of effect of truncation error and rounding errors.
2. Euler shows the shortest execution time (see Table 3) but also has the highest error (see Table 4).
3. Heun and RK4 demonstrate comparable error margins (see Table 3), but Heun needs less computational time than RK4 (Table 4), making Heun as the most efficient method for this case.

The author's suggestion for future researchers to explore alternative numerical methods such as Adam-Bashforth-Moulton scheme or adaptive Runge-Kutta, which may offer better accuracy and stability for solving the SEIR model. Additionally, future studies can investigate the stability of the SEIR model and observe sensitivity analyses on its parameters.(2014)

REFERENCE

Bronson, R., & Costa, G. (2006). *Schaum's Outline of Differential Equations, Third Edition* (Third). The McGraw-Hill Companies, Inc.

Chapra, S. C., & Canale, R. P. (2015). *Numerical Methods for Engineers* (7th Edition). McGraw-Hill Education.

Charostad, J., Rezaei Zadeh Rukerd, M., Mahmoudvand, S., Bashash, D., Hashemi, S. M. A., Nakhaie, M., & Zandi, K. (2023). A comprehensive review of highly pathogenic avian influenza (HPAI) H5N1: An imminent threat at doorstep. *Travel Medicine and Infectious Disease*, *55*, 102638. https://doi.org/10.1016/j.tmaid.2023.102638

EVİRGEN, F., UÇAR, E., UÇAR, S., & ÖZDEMİR, N. (2023). Modelling Influenza A disease dynamics under Caputo-Fabrizio fractional derivative with distinct contact rates. *Mathematical Modelling and Numerical Simulation with Applications*, *3*(1), 58–73. https://doi.org/10.53391/mmnsa.1274004

Gourram, H., Baroudi, M., Labzai, A., & Belam, M. (2023). Mathematical modeling and optimal control strategy for the influenza (H5N1). *Communications in Mathematical Biology and Neuroscience*. https://doi.org/10.28919/cmbn/8199

Griggs, E. P., Flannery, B., Foppa, I. M., Gaglani, M., Murthy, K., Jackson, M. L., Jackson, L. A., Belongia, E. A., McLean, H. Q., Martin, E. T., Monto, A. S., Zimmerman, R. K., Balasubramani, G. K., Chung, J. R., & Patel, M. (2022). Role of Age in the Spread of Influenza, 2011–2019: Data From the US Influenza Vaccine Effectiveness Network. *American Journal of Epidemiology*, *191*(3), 465–471. https://doi.org/10.1093/aje/kwab205

Hurit, R. U., & Sudi Mungkasi. (2021). The Euler, Heun, and Fourth Order Runge-Kutta Solutions to SEIR Model for the Spread of Meningitis Disease. *Mathline : Jurnal Matematika Dan Pendidikan Matematika*, *6*(2), 140–153. https://doi.org/10.31943/mathline.v6i2.176

H.V, W. (2014). Before the Vaccines: Medical Treatments of Acute Paralysis in the 1916 New York

Epidemic of Poliomyelitis. *The Open Microbiology Journal*, *8*(1), 144–147. https://doi.org/10.2174/1874285801408010144

Jester, B. J., Uyeki, T. M., & Jernigan, D. B. (2020). Fifty Years of Influenza A(H3N2) Following the Pandemic of 1968. *American Journal of Public Health*, *110*(5), 669–676. https://doi.org/10.2105/AJPH.2019.305557

Kamorudeen, R. T., Adedokun, K. A., & Olarinmoye, A. O. (2020). Ebola outbreak in West Africa, 2014 – 2016: Epidemic timeline, differential diagnoses, determining factors, and lessons for future response. *Journal of Infection and Public Health*, *13*(7), 956–962. https://doi.org/10.1016/j.jiph.2020.03.014

Kharis, M., & Cahyono, A. (2015). PEMODELAN MATEMATIKA PADA EPIDEMI INFLUENZA DENGAN STRATEGI VAKSINASI. *Indonesian Journal of Mathematics and Natural Sciences*, *38*(2), 176–185.

Krishnapriya, P., Pitchaimani, M., & Witten, T. M. (2017). Mathematical analysis of an influenza A epidemic model with discrete delay. *Journal of Computational and Applied Mathematics*, *324*, 155–172. https://doi.org/10.1016/j.cam.2017.04.030

Liang, Y. (2023). Pathogenicity and virulence of influenza. *Virulence*, *14*(1). https://doi.org/10.1080/21505594.2023.2223057

Ludji, D. G., & Buan, F. C. H. (2023). Penerapan Metode Runge-Kutta Orde 4 pada Pemodelan Penularan Penyakit Cacar Monyet. *Jurnal Saintek Lahan Kering*, *5*(2), 24–26. https://doi.org/10.32938/slk.v5i2.1981

Martini, M., Gazzaniga, V., Bragazzi, N., & Barberis, I. (2019). The Spanish Influenza Pandemic: a lesson from history 100 years after 1918. *Journal of Preventive Medicine and Hygiene*, *60*(1), 64–67.

Mena, I., Nelson, M. I., Quezada-Monroy, F., Dutta, J., Cortes-Fernández, R., Lara-Puente, J. H., Castro-Peralta, F., Cunha, L. F., Trovão, N. S., Lozano-Dubernard, B., Rambaut, A., van Bakel, H., & García-Sastre, A. (2016). Origins of the 2009 H1N1 influenza pandemic in swine in Mexico. *ELife*, *5*. https://doi.org/10.7554/eLife.16777

Moghadami, M. (2017). A Narrative Review of Influenza: A Seasonal and Pandemic Disease. *Iranian Journal of Medical Sciences*, *42*(1), 2–13.

Mohammed, S. J., & Mohammed, M. A. (2021). Runge-kutta Numerical Method for Solving Nonlinear Influenza Model. *Journal of Physics: Conference Series*, *1879*(3), 032040. https://doi.org/10.1088/1742-6596/1879/3/032040

Munir, R. (2021). *METODE NUMERIK : Revisi kelima* (Revisi ke-5). Informatika.

Novalia, E., & Nasution, H. (2018). Menguji Kestabilan dan Kekonsistenan Metode Heun Pada Model Epidemi Susceptible, Exposed, Infected and Recovered Untuk Penyakit Demam Berdarah Dengue. *Jurnal Sains Indonesia*, *42*(2), 52–58.

Pratiwi, C. D., & Mungkasi, S. (2021). *Euler's and Heun's numerical solutions to a mathematical model of the spread of COVID-19*. 030110. https://doi.org/10.1063/5.0052915

Rahmadhania, I., & Arif, D. K. (2020). Kontrol Optimal pada Model Penyebaran Virus Influenza Tipe A H1N1 dengan Menggunakan Prinsip Minumum Pontryagin. *Limits: Journal of Mathematics and Its Applications*, *17*(1), 67. https://doi.org/10.12962/limits.v17i1.6694

Richard, M., & Fouchier, R. A. M. (2016). Influenza A virus transmission via respiratory aerosols or droplets as it relates to pandemic potential. *FEMS Microbiology Reviews*, *40*(1), 68–85. https://doi.org/10.1093/femsre/fuv039

Setiawan, L. I., & Mungkasi, S. (2021). PENYELESAIAN MODEL EPIDEMI SIR MENGGUNAKAN

METODE RUNGE-KUTTA ORDE EMPAT DAN METODE ADAMS-BASHFORTH-MOULTON. *Komputasi: Jurnal Ilmiah Ilmu Komputer Dan Matematika*, *18*(2), 55–61. https://doi.org/10.33751/komputasi.v18i2.3623

The Lancet. (2017). The global HIV/AIDS epidemic—progress and challenges. *The Lancet*, *390*(10092), 333. https://doi.org/10.1016/S0140-6736(17)31920-7

Wu, Y.-C., Chen, C.-S., & Chan, Y.-J. (2020). The outbreak of COVID-19: An overview. *Journal of the Chinese Medical Association*, *83*(3), 217–220. https://doi.org/10.1097/JCMA.0000000000000270